TRPA1 is a candidate for the mechanosensitive transduction channel of vertebrate hair cells

David P. Corey[1,2]*, Jaime García-Añoveros[4]*, Jeffrey R. Holt[5]*, Kelvin Y. Kwan[1,2]*, Shuh-Yow Lin[1,6]*, Melissa A. Vollrath[1,2]*, Andrea Amalfitano[8], Eunice L.-M. Cheung[1], Bruce H. Derfler[1,2], Anne Duggan[4], Gwénaëlle S. G. Géléoc[5], Paul A. Gray[1,3], Matthew P. Hoffman[9], Heidi L. Rehm[7], Daniel Tamasauskas[1,2] & Duan-Sun Zhang[1,2]

[1]*Department of Neurobiology and* [2]*Howard Hughes Medical Institute, Harvard Medical School, and* [3]*Dana-Farber Cancer Institute, Boston, Massachusetts 02115, USA*
[4]*Departments of Anesthesiology, Neurology and Physiology, Northwestern University Institute for Neurosciences, Chicago, Illinois 60611, USA*
[5]*Departments of Neuroscience and Otolaryngology, University of Virginia School of Medicine, Charlottesville, Virginia 22908, USA*
[6]*Department of Biology, Massachusetts Institute of Technology, and* [7]*Laboratory for Molecular Medicine, Harvard-Partners Genome Center, Cambridge, Massachusetts 02139, USA*
[8]*Department of Pediatrics, Division of Medical Genetics, Duke University Medical Center, Durham, North Carolina 27705, USA*
[9]*Matrix and Morphogenesis Unit, CDBRB, NIDCR, NIH, Bethesda, Maryland 20892, USA*

* These authors contributed equally to this work

Mechanical deflection of the sensory hair bundles of receptor cells in the inner ear causes ion channels located at the tips of the bundle to open, thereby initiating the perception of sound. Although some protein constituents of the transduction apparatus are known, the mechanically gated transduction channels have not been identified in higher vertebrates. Here, we investigate TRP (transient receptor potential) ion channels as candidates and find one, TRPA1 (also known as ANKTM1), that meets criteria for the transduction channel. The appearance of TRPA1 messenger RNA expression in hair cell epithelia coincides developmentally with the onset of mechanosensitivity. Antibodies to TRPA1 label hair bundles, especially at their tips, and tip labelling disappears when the transduction apparatus is chemically disrupted. Inhibition of TRPA1 protein expression in zebrafish and mouse inner ears inhibits receptor cell function, as assessed with electrical recording and with accumulation of a channel-permeant fluorescent dye. TRPA1 is probably a component of the transduction channel itself.

Positive deflection of the mechanosensitive stereocilia bundle of vertebrate hair cells opens ion channels in the tips of the stereocilia[1,2]. The extraordinary speed of channel opening after bundle deflection suggested that these transduction channels are directly gated by mechanical force on the channel protein, and that such channels represent a novel group of ion channels that are mechanically gated[3,4]. Since then, a variety of mechanically gated ion-channel proteins have been identified in other systems[5]; however, the hair-cell transduction channel has remained elusive. The difficulty stems in no small part from the relative scarcity of the channel protein in the inner ear: each cell has only a few hundred functional transduction channels, largely precluding biochemical analysis.

Physiology has provided some clues: the transduction channel is a non-selective cation channel with a high Ca^{2+} permeability and ~100 pS conductance. It is permeable to some small organic cations and, remarkably, to the fluorescent lipophilic dye FM1-43 (refs 6–8). Whereas these characteristics rule out candidate channels of the DEG/ENaC family, which may mediate touch sensation in nematodes[9], they are typical of ion channels of the TRP superfamily[8,10,11]. Moreover, TRP channels are found in a variety of sense organs, probably mediating pheromone transduction (TRPC2), sweet and bitter taste (TRPM5), warm and cool thermal sensation (TRPV1–4, TRPM8, TRPA1), insect vision (TRP, TRPL, TRPL-γ), insect touch (NOMPC), and insect hearing (Nanchung)[12,13]. The TRPN (also known as NOMPC) channels in *Drosophila* bristle organs have the same speed and sensitivity as the hair-cell channel[14], and its homologue in zebrafish participates in hair-cell function[15]. Yet mammalian genomes apparently lack TRPN1.

To find transduction channel candidates, we searched a variety of genomes and identified channels within the TRP superfamily. *In situ* hybridization in the mouse inner ear for all mouse TRPs revealed significant expression of TRPA1, a channel activated by mustard and cinnamon oils and by cold[16–18]. We found that TRPA1 mRNA appears in the inner ear coincident with the onset of mechanotransduction, that antibodies to TRPA1 co-localize with the transduction apparatus, and that disruption of TRPA1 in zebrafish and mouse inhibits hair-cell transduction. The TRPA1 protein may thus be a subunit of the transduction channel itself.

In situ hybridization

The mouse genome encodes 33 ion channels of the TRP superfamily (M. Gupta, H.L.R., A.D. and D.P.C., unpublished results). To identify candidates for the vertebrate hair-cell transduction channel, we constructed *in situ* hybridization probes for all 33, and looked for expression in neonatal mouse inner ear. Three different probes for the mouse TRPA1 ion channel (mmTRPA1) strongly labelled the organ of Corti of the cochlea, which contains the auditory hair cells (Fig. 1a, c). To mark hair cells we also used an *in situ* probe to Math1 (Fig. 1b, d), a transcription factor essential for hair-cell specification[19]. Cochlear hair cells were lightly labelled with the *in situ* probe for TRPA1 (Fig. 1c), whereas stronger label appeared in Hensen's cells, a type of supporting cell adjacent to hair cells. Hair cells of the mouse saccule (Fig. 1e) and semicircular canals (not shown) were also lightly labelled with the TRPA1 probes. Although labelling was not very strong in hair cells, this might be expected if the transduction channel is present at a few hundred copies per cell. Probes for other TRP channels (except for TRPML3; see ref. 20) did not label hair cells above background levels.

Expression during development

If TRPA1 participates in hair-cell transduction, its mRNA should appear just before hair cells become mechanically sensitive. The first

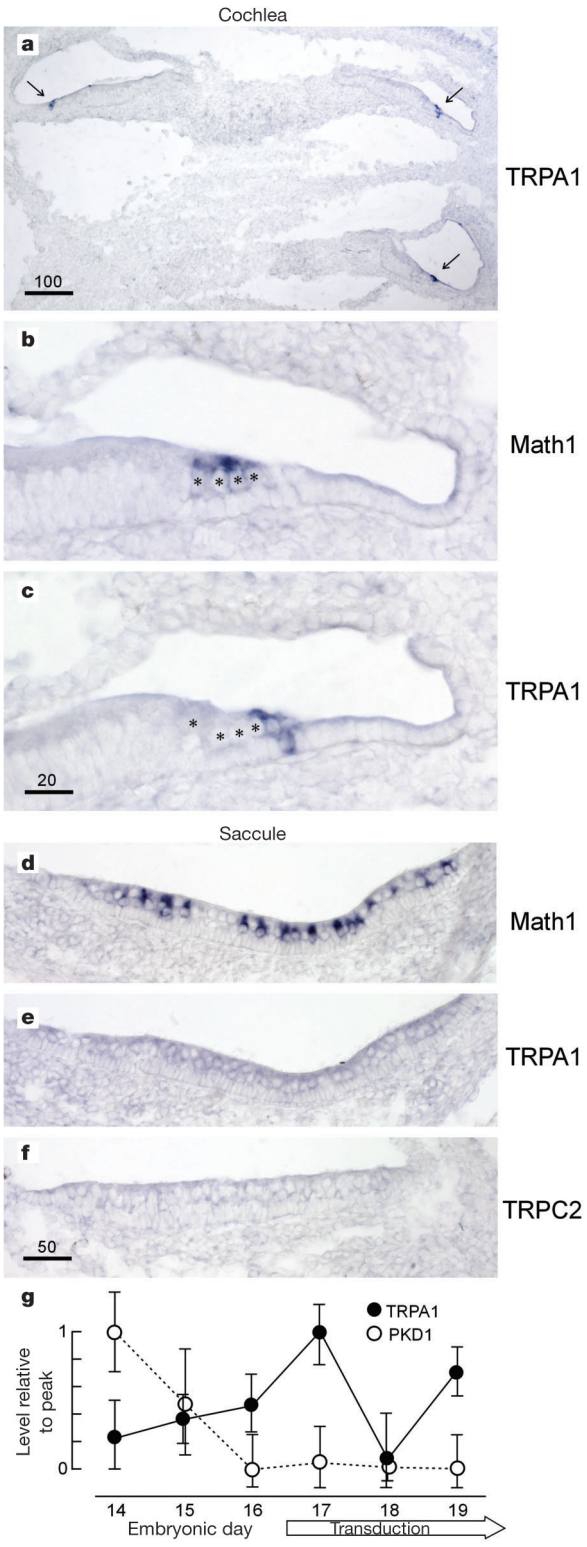

Figure 1 Expression of TRPA1 in the mouse inner ear. **a**, *In situ* hybridization at P0 for TRPA1 in cochlea (probe 194–1,020 bp). Arrows mark organ of Corti. **b**, *In situ* hybridization for Math1 in organ of Corti hair cells (asterisks). **c**, TRPA1, section adjacent to **b**. Hensen's cells are strongly labelled. **d**, Math1 in the mouse saccule. **e**, TRPA1, section adjacent to **d**. Hair cells are faintly labelled. **f**, TRPC2 as a negative control. **g**, Quantitative RT–PCR for TRPA1 and PKD1 during development. TRPA1 message rises just before the onset of transduction at E17. Data are mean ± s.d.; $N = 6$. Scale bars are in micrometres.

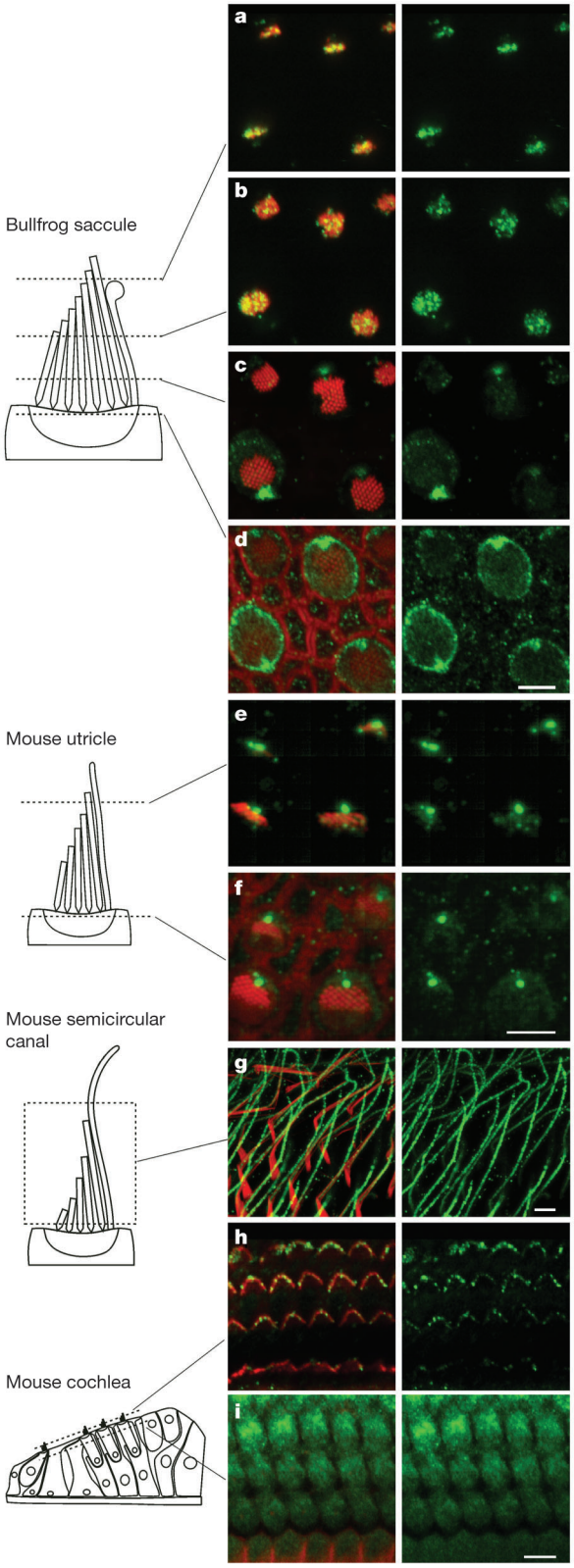

Figure 2 Antibody labelling of TRPA1 in bullfrog and mouse inner ears. Red, actin; green, TRPA1 antibody 0203mt. Right panel is TRPA1 antibody alone. **a**–**d**, Adult bullfrog saccule; optical sections as indicated. **e**, **f**, Hair cells from the mouse utricle; optical sections through a whole mount showing tips or bases of stereocilia. **g**, Hair bundles from the mouse semicircular canal. **h**, Hair cells from the mouse cochlea at P7. **i**, Label also appears in the cell bodies of hair cells. Scale bar, 5 μm.

NATURE | doi:10.1038/nature03066 | www.nature.com/nature

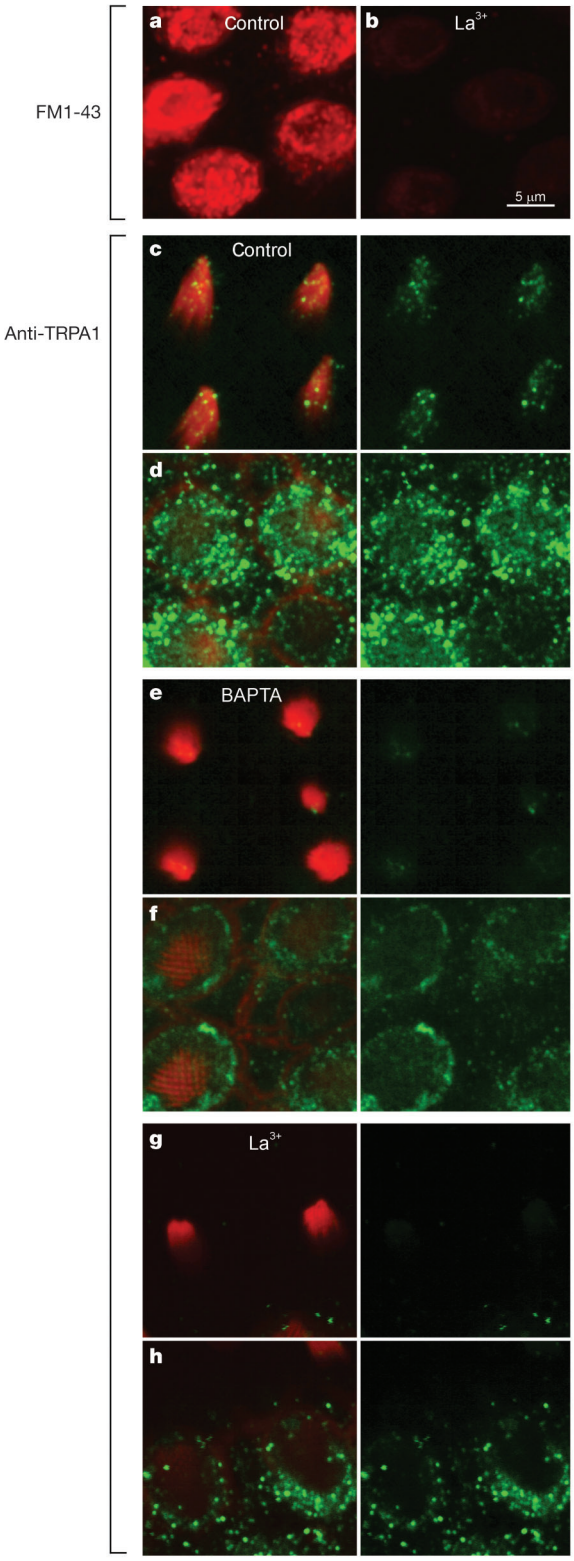

Figure 3 Redistribution of TRPA1 label upon disruption of the transduction apparatus. **a**, Accumulation of FM1-43 (red) in bullfrog hair cells during a 3-min exposure to the dye; optical section through the cell bodies. **b**, After treatment with 5 mM La^{3+} for 20 min. **c**, TRPA1 label (green) and actin label (red) in hair bundles of bullfrog hair cells. Average of two optical sections through the distal 3 μm of the bundles. **d**, Optical sections through the cuticular plate region showing the pericuticular zone. **e**, **f**, After treatment with 5 mM BAPTA for 20 min before fixation. **g**, **h**, After treatment with 5 mM La^{3+} for 20 min before fixation.

wave of mouse utricular hair cells, generated at embryonic day (E)12–13, acquires functional transduction at E17 (ref. 21). We used quantitative polymerase chain reaction with reverse transcription (RT–PCR) to assess message for several TRP channels during development of the mouse utricle (Fig. 1g). TRPA1 message was first detected at E15 and E16, and peaked at E17. Message level dropped at E18, but then rose again at E19, possibly corresponding to a second wave of hair cells that are generated at about E15 (ref. 22) and transduce by E19 (G.S.G.G. and J.R.H., unpublished data).

Antibody labelling

We raised antibodies to the carboxy terminus of mmTRPA1, after the sixth predicted transmembrane domain (Supplementary Fig. S1a). Antisera were affinity purified against either the entire C terminus (antibody 0203mt) or a small peptide representing conserved sequences within it (0203f1). In immunoblots, both the TRPA1 antibody (0203mt) and an antibody to green fluorescent protein (GFP) labelled a GFP::mmTRPA1 fusion protein expressed in HEK293 cells, indicating that our antibody recognizes the TRPA1 protein (Supplementary Fig. S2a).

Two other components of the transduction apparatus—myosin 1c (the adaptation motor) and cadherin 23 (a tip-link protein)—are located at the tips of the stereocilia, throughout the kinocilium and in the pericuticular zone (a vesicle-rich region of the apical surface)[23,24]. To see whether TRPA1 was similarly located, we first looked in hair cells of the bullfrog saccule, whose large hair bundles facilitate antibody localization. TRPA1 immunoreactivity (antibody 0203mt) was found in the distal half of the stereocilia and along the length of the kinocilium (Fig. 2a, b). It was scarce or absent in the proximal part of the stereocilia (Fig. 2c), but strong in the pericuticular zone (Fig. 2d). Lighter labelling was also observed in the cell bodies of hair cells, but not supporting cells. We found a very similar labelling pattern with an alternatively purified antibody (0203f1; Supplementary Fig. S2g, h). Label was absent when the primary antibody was absent or when it had been pre-absorbed against the antigen (Supplementary Fig S2e, f, i, j).

In hair cells of the mouse vestibular system stereocilia labelling was light, whereas the kinocilium and pericuticular zone were consistently labelled (Fig. 2e, f). The long kinocilia of semicircular canal hair cells showed robust label (Fig. 2g). In inner and outer hair cells of the mouse cochlea, immunoreactivity was strongest in the apical region of the hair cells but appeared lower in cell bodies as well (Fig. 2h, i). Labelling of the stereocilia tips was seen (Fig. 2h), especially in animals older than postnatal day 4 (P4), but was difficult to distinguish from cell body labelling in these short stereocilia. Kinocilia were consistently labelled at P3–P5. In Hensen's cells of the cochlea, where the *in situ* label was strongest, the Golgi apparatus was brightly labelled (Supplementary Fig. S4), further supporting the specificity of the antibody.

Because the tip link protein cadherin 23 is also present in retinal photoreceptors[25], we asked whether TRPA1 might be in photoreceptors. Indeed, in immunoblots of bullfrog retina, the TRPA1 antibody recognizes a single prominent band of the predicted molecular mass, and in sections TRPA1 immunoreactivity was found in the outer and inner segments of bullfrog photoreceptors (Supplementary Fig. S4).

In hair cells, tip links can be removed and mechanosensitivity abolished by a short treatment with La^{3+} ions or the Ca^{2+} chelator BAPTA[26,24]. Notably, cadherin 23 immunoreactivity disappears from the stereocilia within 20 min after either treatment, suggesting that the transduction complex is rapidly recycled when damaged[24]. If TRPA1 is part of the transduction complex, we might expect similar redistribution after disruption of the tip link. We first confirmed that La^{3+} and BAPTA abolish transduction channel function. Treatment of bullfrog saccular hair cells with either reagent prevented accumulation of the small fluorescent dye FM1-43, which passes through open hair-cell transduction channels

and is trapped in cytoplasm[7,8]. La^{3+} was more effective, almost completely eliminating FM1-43 labelling in all hair cells, whereas hair cells at the edge of the sensory epithelium resisted BAPTA treatment (Fig. 3a, b).

We then treated bullfrog saccules with either BAPTA or La^{3+} and followed TRPA1 redistribution with the 0203mt antibody. Both treatments caused substantial loss of TRPA1 immunoreactivity from the tips of stereocilia, reducing the levels of label by 75–85% (Fig. 3c–h). Immunoreactivity in the pericuticular zone was also reduced by La^{3+} (Fig. 3g, h), a pattern strikingly similar to that of the tip-link protein.

Morpholino oligonucleotides in zebrafish

We wondered whether inhibiting TRPA1 expression reduced transduction channel function. In zebrafish, protein expression can be inhibited by injection of morpholino oligonucleotides (morpholinos) into early embryos. We first identified zebrafish homologues of TRPA1 from partial sequences in the *Danio rerio* genome. There are two, consistent with the duplication of the zebrafish genome, which we designate *trpa1* and *trpa2* (encoding drTRPA1 and drTRPA2, respectively). We determined the full-length coding sequences of both by PCR amplification from zebrafish complementary DNA and 5′ and 3′ rapid amplification of cloned ends (RACE) (Supplementary Fig. S1a, b). The drTRPAs are most closely related to each other and to a TRPA from the puffer fish, and are much more similar to channels of the TRPA branch than to any other TRP superfamily branch. To determine the exon structures of these genes, we compared their cDNA sequences to zebrafish genomic sequence (Supplementary Fig. S3, and data not shown).

Morpholinos expected to inhibit the translation or splicing of

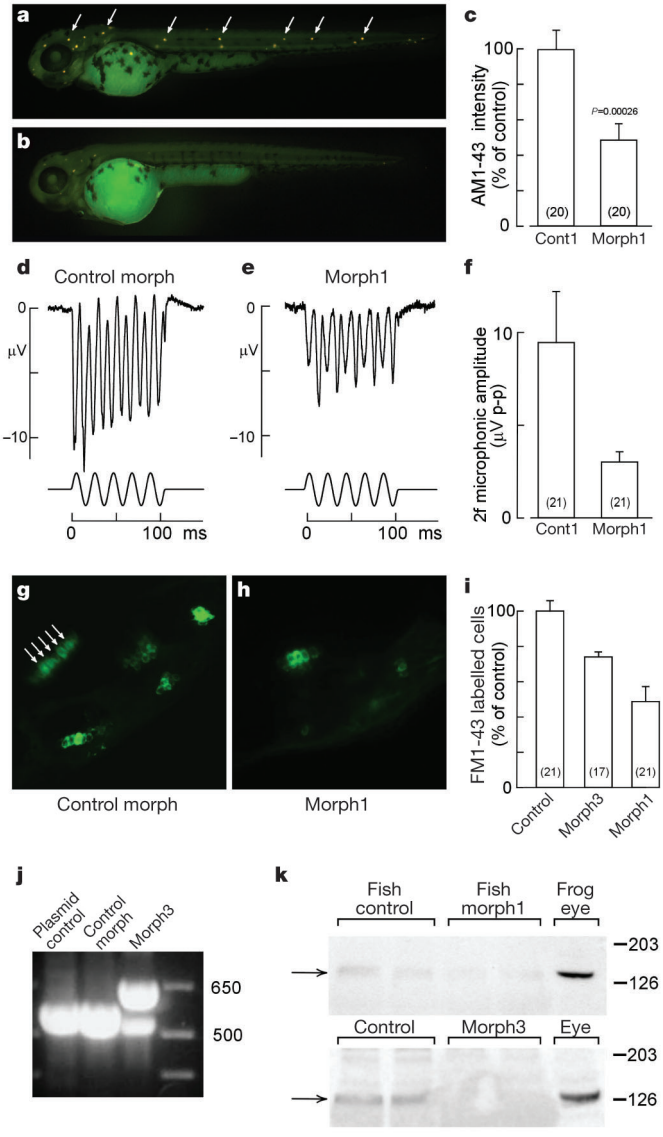

Figure 4 Inhibition of transduction in zebrafish by morpholinos. **a**, AM1-43 in lateral line hair cells (arrows); 60 h.p.f. embryo injected with control morpholino. **b**, Labelling of a 60 h.p.f. embryo injected with morph1. **c**, Total AM1-43 intensity in fish neuromasts. Data are mean ± s.e.m., $N = 20$, $P < 0.0003$. **d**, Microphonic potential in the otocyst of a control-injected fish. **e**, Fish injected with morph1. **f**, Summary of microphonic potentials; peak-to-peak (p-p) amplitude at twice the stimulus frequency (2f). Data are mean ± s.e.m., $N = 21$, $P < 0.03$. **g**, FM1-43 in zebrafish inner ear hair cells (arrows) after dye injection into the otocyst. Projection of ~40 optical sections through a control-morpholino-injected zebrafish at 55 h.p.f. **h**, Otocyst of a morph1-injected zebrafish. **i**, Summary of FM1-43-labelled hair cells. Data are mean ± s.e.m. **j**, RT–PCR of control plasmid and morpholino-injected embryos (60 h.p.f.). **k**, Immunoblot of whole 60 h.p.f. embryos injected with control morpholino, morph1 or morph3; bullfrog eye is positive control. Numbers along the right are bases in **j** and kDa in **k**.

NATURE | doi:10.1038/nature03066 | www.nature.com/nature

mRNA for drTRPA1 and drTRPA2, as well as a standard control morpholino, were injected into zebrafish embryos at the one-cell stage. Hair cells of the zebrafish inner ear and lateral line become functional beginning at about 48 h post-fertilization (h.p.f.). After ~70 h.p.f., dilution and degradation of morpholinos apparently allow recovery from suppression and cause variability in morphant phenotypes[15]. We therefore tested hair-cell function between 58 and 72 h.p.f.

To assay lateral line hair cells, we bathed zebrafish embryos (60 h.p.f.) for 5 min in water containing FM1-43 or AM1-43 (a fixable analogue). Uninjected embryos and those injected with control morpholino showed brightly labelled hair cells (Fig. 4a). Fish injected with two different morpholinos targeting drTRPA2 were also labelled (data not shown), suggesting that drTRPA2 is not involved in hair-cell transduction. However, fish embryos injected with morpholinos targeting drTRPA1's translation initiation site (morph1) or a splice junction (morph3) showed neuromast fluorescence reduced to 44 ± 9% of controls (mean ± s.e.m., $N = 20$, $P < 0.0001$) or 74 ± 3% of controls ($N = 17$, $P < 0.0001$), respectively (Fig. 4b, c). DrTRPA1 is apparently necessary for the complete function or development of embryonic lateral line hair cells.

To assay inner ear hair cells of fish, we recorded the otocyst microphonic potential, an extracellular voltage resulting from current flow through transduction channels. Vibration of a stimulus pipette placed near the otocyst evoked a negative-going potential at twice the stimulus frequency (Fig. 4d), as expected if the stimulus alternately excited hair cells of opposite orientations. The potential became saturated for large amplitudes and its peak occurred slightly before the stimulus peak, as expected for hair cells; furthermore, it was abolished by the channel blocker streptomycin in the recording pipette. Fish embryos (58–70 h.p.f.) injected with a control morpholino consistently showed robust, stimulus-evoked microphonic potentials, whereas those injected with morph1 had potentials 32 ± 5% that of controls ($N = 21$, $P < 0.03$) (Fig. 4e, f).

Injection of morph1 and morph3 also reduced FM1-43 accumulation in inner ear hair cells. After physiological recording, we pressure-ejected a small amount of pipette solution, which contained FM1-43, into the otocyst. FM1-43 entered hair cells (but not other cells) within 2–3 min. Individual dye-labelled hair cells were counted in three-dimensional confocal reconstructions of each otocyst (Fig. 4g). About 30 hair cells were labelled with dye in control fish, but fewer were labelled in morph1- or morph3-injected fish (49 ± 8% of control, $N = 21$, $P < 0.00001$ and 74 ± 4%, $N = 17$, $P < 0.0001$, respectively). FM1-43 intensity in each cell also appeared lower than in controls.

To test whether the morpholinos had simply delayed hair-cell development, we fixed each dye-labelled embryo after confocal imaging. Permeablization with acetone allowed FM1-43 to diffuse from hair cells. Hair bundles were labelled with fluorescent phalloidin, and the confocal reconstructions repeated. Control otocysts had 58 ± 2.5 hair cells with bundles, whereas morph1-injected fish had only slightly fewer (51 ± 2.5, $N = 19$). Thus, the inhibitory effect of morph1 on transduction cannot be explained by fewer hair cells in the inner ear.

Finally, to confirm that the morpholinos did in fact disrupt drTRPA1 mRNA splicing and reduce protein levels, we extracted total RNA and protein from ~60 h.p.f. embryos injected with experimental and control morpholinos. By sequencing RT–PCR products, we found that morph3 caused a frameshift mutation and a stop codon insertion before drTRPA1's transmembrane domains by blocking splicing of intron 20–21 or by using a cryptic splicing donor site 22 base pairs (bp) 5′ to the normal donor site (Fig. 4j). In immunoblots with antibody 0203mt we confirmed that the level of intact drTRPA1 protein was much reduced in both morph1- and morph3-injected embryos (Fig. 4k).

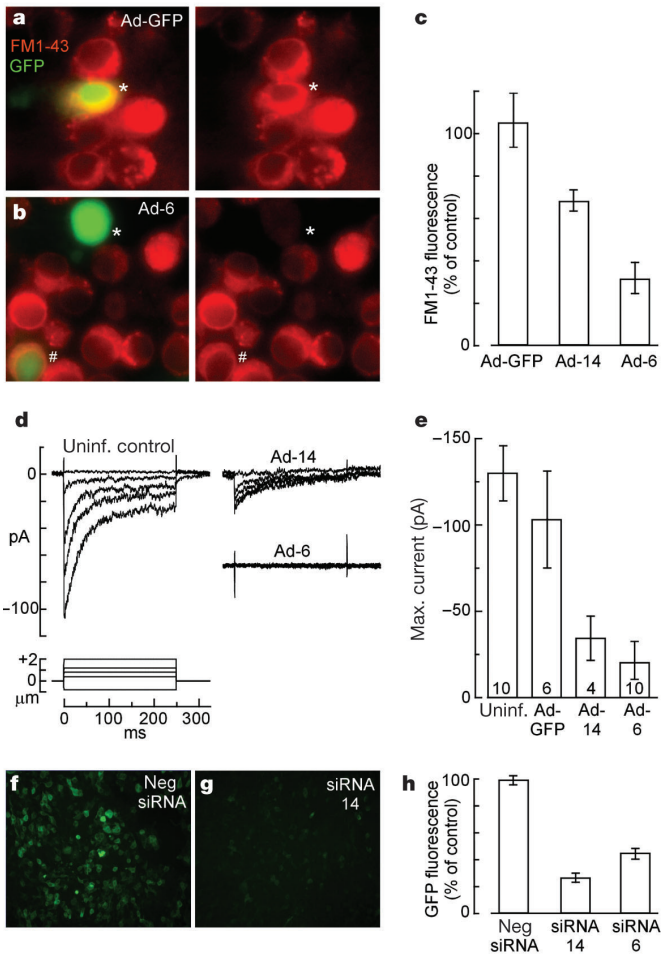

Figure 5 Inhibition of transduction in mouse with adenoviruses encoding siRNAs. **a**, Utricular hair cells labelled with FM1-43 to mark transducing cells; optical section through the cell body. A hair cell (asterisk) infected with Ad-GFP (green) accumulated FM1-43. **b**, Ad-6-infected cells are green; only one (hash) accumulated FM1-43. **c**, Summary of FM1-43 accumulation in infected cells (average intensity per cell) relative to uninfected controls. Data are mean ± s.e.m. **d**, Typical transduction currents in uninfected cells and cells infected with Ad-14 or Ad-6. **e**, Summary of peak currents. Data are mean ± s.e.m., *N* is as indicated. **f**, HEK cells transfected with GFP::mmTRPA1 and a negative control siRNA construct. **g**, HEK cells transfected with GFP::mmTRPA1 and siRNA-14. **h**, Green fluorescence intensity above background, with co-transfection with the control siRNA, siRNA-14, or siRNA-6. Data are mean ± s.d.; $N = 5$.

Small interfering RNAs in mouse

To disrupt *Trpa1* expression in mouse hair cells, we designed two hairpin small interfering (si)RNAs targeting mmTRPA1 (siRNA-6 and siRNA-14; Supplementary Fig. S1a) and placed them under the control of the H1 promoter in the pSUPER vector, which were then inserted into adenoviruses. Although adenoviruses readily infect hair cells, first generation replication-incompetent adenoviruses have sufficient toxicity to damage hair bundles and disrupt transduction[27]. To avoid such toxicity we developed an adenoviral vector that is multiply deleted of the E1, polymerase and pTP genes[28], and that—unlike first generation adenoviruses—does not damage hair-cell transduction even many days after infection[29,30].

When mRNA is cleaved by introduction of siRNAs after differentiation, function is not lost until the endogenous protein product has been degraded. We reasoned that we could disrupt TRPA1 function without delay if we infected cells before the TRPA1 channels are normally synthesized. Transduction in hair cells of the mouse utricle normally appears at E17 (ref. 21), so we cultured

utricles from mice at E15, infected them with adenoviruses in culture at E16, and studied the cells at E17–E20.

We first asked whether the siRNAs inhibited FM1-43 accumulation. The adenoviruses also encoded GFP and so infected cells were fluorescent and could be compared to adjacent, uninfected control cells. Cells infected with adenoviruses encoding either siRNA (Ad-6 and Ad-14) displayed diminished FM1-43 fluorescence compared with controls, but cells infected with the same adenovirus encoding GFP alone (Ad-GFP) did not (Fig. 5a–c).

With whole-cell patch clamping, we then recorded the transduction current from infected and control cells. Uninfected cells had transduction currents of 100–150 pA, and cells infected with Ad-GFP had transduction currents not significantly lower (Fig. 5d, e). However, cells infected with adenoviruses encoding siRNAs had currents significantly smaller than either uninfected or Ad-GFP-infected controls ($P < 0.04$; Fig. 5d, e). We did not detect a change in other aspects of the response, for instance in the time course of adaptation or the resting position of the activation curve. Voltage-activated currents in Ad-6- and Ad-14-infected embryonic cells were indistinguishable from those in uninfected controls, suggesting that the siRNAs primarily reduced the number of functional transduction channels. As a further control for toxicity, we cultured utricles from P3 mice infected with Ad-6, and recorded from infected cells 1–2 days after infection. We reasoned that any adenovirus toxicity would be apparent in this time frame, but that the endogenous TRPA1 protein would not be significantly degraded. Infected cells had a mean transduction current equivalent to uninfected controls at that age (165 ± 29 pA, mean ± s.e.m., $N = 4$), and their current–voltage relations and adaptation were also similar to controls.

Finally, we confirmed that the siRNAs reduce the expression of *Trpa1*. We transfected HEK cells with a plasmid encoding a GFP::mmTRPA1 fusion protein driven by a CMV promoter, and co-transfected these cells with plasmids encoding siRNA-6, siRNA-14, or a negative control siRNA sequence. Green fluorescence, indicating expression of the GFP::mmTRPA1 fusion, was significantly reduced when cells were co-transfected with either siRNA-6 or siRNA-14 compared with the control siRNA. In infected utricles, the low infection rate precluded analysis by immunoblot or RT–PCR; however, we often observed that hair cells infected with Ad-6 had little or no TRPA1 immunoreactivity compared with uninfected neighbours (Supplementary Fig. S2b).

Discussion

A variety of evidence supports the idea that TRPA1 is a component of the mechanosensitive transduction channel of vertebrate hair cells. The level of TRPA1 mRNA increases markedly in the mouse utricle at E17, the same developmental stage at which transduction appears in utricular hair cells. Antibodies to TRPA1 label the stereocilia, kinocilia and the pericuticular zone of hair cells in both bullfrog and mouse. Although antibody label was not always strong in stereocilia of mouse hair cells, it did match immunoreactivity reported for two other components of the transduction apparatus—cadherin 23 and myosin 1c—which are at the tips of stereocilia but also present throughout kinocilia[23,24]. Moreover, labelling disappeared from the hair bundles within minutes during treatment with La^{3+} or the Ca^{2+} chelator BAPTA, which break tip links and cause similar redistribution of the tip-link protein cadherin 23 (ref. 24).

Additional support comes from inhibiting *Trpa1* expression in zebrafish and mouse. Two different morpholino oligonucleotides directed against zebrafish TRPA1 reduced transduction channel function, as measured both with accumulation of FM1-43 and with microphonic potential responses. Morpholino-injected fish had nearly normal numbers of hair bundles, arguing against an indirect developmental effect. In mouse utricle, two different adenoviruses encoding siRNAs targeting TRPA1 message resulted in decreased FM1-43 accumulation and decreased transduction currents. These siRNA effects were not attributable to adenovirus toxicity. Finally, the transduction channel of turtle and mouse hair cells is blocked by 5–10 μM of ruthenium red (ref. 31; J.R.H., data not shown), similar to the block of TRPA1 channels expressed in bullfrog oocytes. It seems most likely that TRPA1 is a component of the hair-cell transduction channel itself.

What is the role of the TRPN1 (or NOMPC) channel, which is also necessary for hair-cell transduction in zebrafish[15]? Perhaps TRPA1 and TRPN1 form heteromultimeric channels in zebrafish, with both necessary for transduction. Perhaps, instead, individual hair cells use either TRPA1 or TRPN1, but not both. Whatever the case in zebrafish, TRPA1 is the only good candidate for the mechanosensitive transduction channel of mammalian hair cells, as the genomes of mammals lack TRPN1 (data not shown).

TRPA1 is also reportedly activated by cold and by compounds such as horseradish, mustard oil, cinnamon oil and cannabinoids[16–18]. The variety of agonists suggests a number of receptors coupled to TRPA1 by second messengers; the mechanical activation of the hair-cell transduction channel is, however, far too fast to involve a second messenger[3]. Many small-diameter neurons in dorsal root ganglia express TRPA1, suggesting a role in chemical nociception. Perhaps TRPA1 in sensory neurons is activated by a variety of painful stimuli, both indirectly through associated receptors and directly by strong mechanical force.

TRPA1 and TRPN1 (NOMPC) are unique among the TRP channel superfamily in possessing a large number of ankyrin domains in their amino termini (17 and 29, respectively). Moreover, the TRPA and TRPN branches of the family are not closely related phylogenetically[13], and the ankyrin domains of each are no more similar to each other than they are to the multiple ankyrin domains of the three ankyrin genes. This argues for elaboration of the ankyrin domains in these two TRPs as a case of convergent evolution, and begs the question of what special function they might serve.

The ankyrin repeats might bind to motor proteins that maintain tension on the channel[32]. If so, we might expect the loop regions of each repeat to be very similar if they bind to many copies of the same motor; instead, the loop sequences are the least conserved part of the ankyrin repeats within TRPA1. Alternatively, the ankyrin repeats might bind other signalling or modulatory proteins. If TRPA1 is most generally a polymodal nociceptor, different receptor proteins could dock at the extended N terminus in different cellular contexts.

Most intriguing, however, is the possibility that tandem ankyrin repeats can form a spring (V. Bennett, personal communication; see also refs 33, 34). Hair-cell transduction channels are in series with a biophysically defined "gating spring" of ~1 mN m^{-1} stiffness[35]. The tip link has been considered to be the gating spring; however, the recent discovery[24,36] that the tip link is composed in large part by cadherin 23, which is probably not very elastic, shifts attention elsewhere[33]. The crystal structure of ankyrin repeats suggests another possibility: the two helices of each repeat pack pairwise to form an extended but curved structure[37]. Molecular dynamics simulations (M. Sotomayor, K. Schulten and D.P.C., unpublished results) suggest that its curvature creates an effective stiffness of a few mN m^{-1}, about the same as that needed for the gating spring. Moreover, they suggest that larger forces can pull apart the packed helices, perhaps serving as a safety release to prevent damage by excessive stimuli. If the ankyrin repeats of TRPA1 form a spring, the tip link could be a relatively stiff linker while the elastic gating spring is intracellular and part of the channel itself[38].

TRPA1, if it is the hair-cell transduction channel, may serve another role in hearing: after channel opening, Ca^{2+} enters and binds to the channel or a nearby site to promote channel closure, a process termed fast adaptation[35,39]. The rapid conformational change associated with channels closing together tightens tip links and moves the hair bundle by several nanometres. It has been suggested that this mechanism, if timed appropriately to different

stimulus frequencies for each hair cell, could amplify the vibration of the cochlea's basilar membrane (a process termed the 'cochlear amplifier') and so mediate frequency tuning for auditory sensation[40]. If so, the TRPA1 protein could be at once the hair-cell transduction channel, the gating spring and the cochlear amplifier. □

Methods

Full methods are available in Supplementary Information.

In situ probes

Segments of cDNA for each TRP channel were amplified by PCR from mouse libraries and cloned into the pCRII-TOPO vector (Invitrogen). TRP channel cDNA flanked by Sp6 and T7 promoters was amplified and used for *in vitro* transcription with digoxigenin-labelled rUTP. Hybridizations on mouse E17 and P0 frozen sections were visualized with anti-DIG F_{ab} conjugated to alkaline phosphatase.

Real-time RT–PCR

Twenty utricular epithelia were excised from embryonic mice, from E14 to E19. DNase-free RNA was prepared (RNAqueous-4PCR; Ambion) and used to make cDNA with TaqMan reagents (Applied Biosystems). Real-time PCR was performed using SYBR Green PCR Master Mix (Applied Biosystems) and an I-Cycler (Bio-Rad). DNase-treated RNA was a negative control and melt curve analysis confirmed that a single product was amplified. Gene expression was normalized to myosin 7a; normalization to S29 gives similar results.

Antibody generation and labelling

Rabbits were immunized with a GST fusion of mouse TRPA1 C terminus. Antibody 0203mt was purified on the mouse C terminus and 0203f1 on a conserved peptide within the zebrafish TRPA1 C terminus. Bullfrog saccules were dissected and their otolithic membranes removed, then either fixed immediately or incubated for 20 min with 5 mM La^{3+}, 5 mM BAPTA, or 0.1 Ca^{2+} before fixation. Cochleae, utricles and semicircular canals from neonatal mice were surgically exposed and fixed *in situ*. Primary antibodies were used at 7–10 $\mu g\,ml^{-1}$.

Zebrafish TRPAs

Fragments of two zebrafish homologues of mouse *Trpa1* were identified in the Ensembl database. RNA was collected from 4–5 d.p.f. zebrafish and cDNA made using SMART RACE cDNA amplification (BD Biosciences). Primers for full-length zebrafish *trpa* genes were based on RACE data and on Ensembl sequence. Exon structures were determined by comparison to genomic sequence in the Ensembl database. The two zebrafish homologues of mouse *Trpa1* are deposited in GenBank under accession numbers AY677196 and AY677197.

Morpholino injections and RT–PCR

Morpholinos targeting drTRPA1, drTRPA2 or a standard control (Gene Tools) were injected into one-cell-stage zebrafish embryos (~2.5 nl; 0.5 mM stock). Embryos were studied at 58–70 h.p.f. Total RNA from 60-h.p.f. embryos was extracted by Trizol, genomic DNA removed by DNase I, and cDNA synthesized by Superscript II (Invitrogen). Nested PCR amplified a drTRPA1 fragment from exon 18 to exon 22, which was sequenced.

Immunoblots

Proteins from morphant embryos (30–40 animals; 58–60 h.p.f.) or four bullfrog eyes were run on a 10–20% gradient SDS gel. DrTRPA1 was detected with antibody 0203mt (1:750) and HRP-conjugated goat anti-rabbit antibody (Jackson Immunoresearch) and visualized with enhanced chemiluminescence (Amersham).

Microphonic recording

Larval zebrafish (48–72 h.p.f.) were anaesthetized and mounted dorsal side up. Bath saline contained tetrodotoxin to reduce twitching. Recording pipettes (2–6 MΩ) were advanced through the swelling near the lateral semicircular canal and placed near the otolith of the posterior macula. Microphonic potentials were elicited with a probe placed just behind the otocysts and vibrated at 5–100 Hz along the rostral–caudal axis. A similar method was recently described[41].

FM1-43 and actin labelling

To label lateral line hair cells, embryos (58–60 h.p.f.) were incubated in AM1-43 (5 μM; 5 min), washed, fixed and photographed with a fluorescence microscope. For quantification, pixel intensity was integrated over each neuromast.

To label inner ear hair cells after microphonic recording, recording pipette solution (containing 40 μM FM1-43; Molecular Probes) was pressure-injected into the otocyst. Dye entered hair cells and extracellular dye diffused from the otocyst for 5–10 min before confocal imaging. Embryos were fixed and permeabilized with acetone to extract residual FM1-43 before labelling with fluorescent phalloidin for additional confocal imaging.

siRNAs

siRNA oligonucleotides, designed for RNA hairpin formation, were cloned into the pSUPER vector under an H1 RNA promoter (OligoEngine). A sub-fragment of the vector was subcloned into the pAdTrack shuttle vector[42]—for H1-driven siRNA expression and CMV-driven GFP expression—which was recombined with the pAdEΔpol, ΔpTP plasmid (derived from pAdEasy[42], but lacking parts of the polymerase gene and the pTP gene) to generate pAdEΔpol, ΔpTP/siRNA + GFP, which was grown in *trans*-complementing C-7 cells[28]. Utricles dissected at E15 (ref. 21) were incubated at 37 °C and exposed to adenoviral vectors for 4–24 h, then washed and maintained at 37 °C for 2–5 days.

Recording and fluorescence imaging in mouse utricle

Utricular hair-cell stimulation and recording were previously described[21]. Infected cells were identified by GFP fluorescence and photographed, FM1-43 was applied (5 μM, 10 s) and cells were photographed using a TRITC filter set.

GFP::TRPA1 expression construct and siRNA testing

Full-length mmTRPA1 cDNA was cloned into the N-terminal GFP TOPO vector (Invitrogen) to generate the plasmid pcDNA3.1GFP::TRPA1. HEK293 cells were co-transfected with this plasmid and with siRNA constructs (Ambion Silencer Express) containing a mouse U6 promoter directing transcription of either a negative control sequence or hairpin sequences corresponding to siRNA-6 and siRNA-14. GFP::TRPA1 expression in transfected cells was assessed 24–48 h after transfection. Total fluorescence in a field was calculated from average pixel intensities.

Received 1 July; accepted 29 September 2004; doi:10.1038/nature03066.
Published online 13 October 2004.

1. Hudspeth, A. J. & Corey, D. P. Sensitivity, polarity, and conductance change in the response of vertebrate hair cells to controlled mechanical stimuli. *Proc. Natl Acad. Sci. USA* **74,** 2407–2411 (1977).
2. Hudspeth, A. J. Extracellular current flow and the site of transduction by vertebrate hair cells. *J. Neurosci.* **2,** 1–10 (1982).
3. Corey, D. P. & Hudspeth, A. J. Response latency of vertebrate hair cells. *Biophys. J.* **26,** 499–506 (1979).
4. Corey, D. P. & Hudspeth, A. J. Kinetics of the receptor current in bullfrog saccular hair cells. *J. Neurosci.* **3,** 962–976 (1983).
5. Sukharev, S. & Corey, D. P. Mechanosensitive channels: multiplicity of families and gating paradigms. *Sci. STKE* **2004,** re4 (2004).
6. Corey, D. P. & Hudspeth, A. J. Ionic basis of the receptor potential in a vertebrate hair cell. *Nature* **281,** 675–677 (1979).
7. Gale, J. E., Marcotti, W., Kennedy, H. J., Kros, C. J. & Richardson, G. P. FM1-43 dye behaves as a permeant blocker of the hair-cell mechanotransducer channel. *J. Neurosci.* **21,** 7013–7025 (2001).
8. Meyers, J. R. *et al.* Lighting up the senses: FM1-43 loading of sensory cells through nonselective ion channels. *J. Neurosci.* **23,** 4054–4065 (2003).
9. García-Añoveros, J., García, J. A., Liu, J.-D. & Corey, D. P. The nematode degenerin UNC-105 forms ion channels that are activated by degeneration- or hypercontraction-causing mutations. *Neuron* **20,** 1231–1241 (1998).
10. Duggan, A., García-Añoveros, J. & Corey, D. P. Insect mechanoreception: What a long, strange TRP it's been. *Curr. Biol.* **10,** R384–R387 (2000).
11. Clapham, D. E., Montell, C., Schultz, G. & Julius, D. International Union of Pharmacology. XLIII. Compendium of voltage-gated ion channels: transient receptor potential channels. *Pharmacol. Rev.* **55,** 591–596 (2003).
12. Clapham, D. E. TRP channels as cellular sensors. *Nature* **426,** 517–524 (2003).
13. Corey, D. P. New TRP channels in hearing and mechanosensation. *Neuron* **39,** 585–588 (2003).
14. Walker, R. G., Willingham, A. T. & Zuker, C. S. A *Drosophila* mechanosensory transduction channel. *Science* **287,** 2229–2234 (2000).
15. Sidi, S., Friedrich, R. W. & Nicolson, T. NompC TRP channel required for vertebrate sensory hair cell mechanotransduction. *Science* **301,** 96–99 (2003).
16. Story, G. M. *et al.* ANKTM1, a TRP-like channel expressed in nociceptive neurons, is activated by cold temperatures. *Cell* **112,** 819–829 (2003).
17. Jordt, S. E. *et al.* Mustard oils and cannabinoids excite sensory nerve fibres through the TRP channel ANKTM1. *Nature* **427,** 260–265 (2004).
18. Bandell, M. *et al.* Noxious cold ion channel TRPA1 is activated by pungent compounds and bradykinin. *Neuron* **41,** 849–857 (2004).
19. Bermingham, N. A. *et al.* Math1: an essential gene for the generation of inner ear hair cells. *Science* **284,** 1837–1841 (1999).
20. Di Palma, F. *et al.* Mutations in Mcoln3 associated with deafness and pigmentation defects in varitint-waddler (Va) mice. *Proc. Natl Acad. Sci. USA* **99,** 14994–14999 (2002).
21. Geleoc, G. S. & Holt, J. R. Developmental acquisition of sensory transduction in hair cells of the mouse inner ear. *Nature Neurosci.* **6,** 1019–1020 (2003).
22. Denman-Johnson, K. & Forge, A. Establishment of hair bundle polarity and orientation in the developing vestibular system of the mouse. *J. Neurocytol.* **28,** 821–835 (1999).
23. Hasson, T. *et al.* Unconventional myosins in inner-ear sensory epithelia. *J. Cell Biol.* **137,** 1287–1307 (1997).
24. Siemens, J. *et al.* Cadherin 23 is a component of the tip link in hair-cell stereocilia. *Nature* **428,** 950–955 (2004).
25. Reiners, J. *et al.* Differential distribution of harmonin isoforms and their possible role in Usher-1 protein complexes in mammalian photoreceptor cells. *Invest. Ophthalmol. Vis. Sci.* **44,** 5006–5015 (2003).
26. Assad, J. A., Shepherd, G. M. & Corey, D. P. Tip-link integrity and mechanical transduction in vertebrate hair cells. *Neuron* **7,** 985–994 (1991).
27. Holt, J. R. *et al.* Functional expression of exogenous proteins in mammalian sensory hair cells infected with adenoviral vectors. *J. Neurophysiol.* **81,** 1881–1888 (1999).
28. Hodges, B. L. *et al.* Multiply deleted [E1, polymerase-, and pTP-] adenovirus vector persists despite deletion of the preterminal protein. *J. Gene Med.* **2,** 250–259 (2000).
29. Luebke, A. E., Steiger, J. D., Hodges, B. L. & Amalfitano, A. A modified adenovirus can transfect cochlear hair cells *in vivo* without compromising cochlear function. *Gene Ther.* **8,** 789–794 (2001).
30. Holt, J. R. Viral-mediated gene transfer to study the molecular physiology of the mammalian inner ear. *Audiol. Neurootol.* **7,** 157–160 (2002).
31. Farris, H. E., LeBlanc, C. L., Goswami, J. & Ricci, A. J. Probing the pore of the auditory hair cell

mechanotransducer channel in turtle. *J. Physiol.* **558,** 769–792 (2004).
32. Gillespie, P. G. & Corey, D. P. Myosin and adaptation by hair cells. *Neuron* **19,** 955–958 (1997).
33. Corey, D. P. & Sotomayor, M. Hearing: tightrope act. *Nature* **428,** 901–903 (2004).
34. Howard, J. & Bechstedt, S. Hypothesis: a helix of ankyrin repeats of the NOMPC-TRP ion channel is the gating spring of mechanoreceptors. *Curr. Biol.* **14,** R224–R226 (2004).
35. Howard, J. & Hudspeth, A. J. Compliance of the hair bundle associated with gating of mechanoelectrical transduction channels in the bullfrog's saccular hair cell. *Neuron* **1,** 189–199 (1988).
36. Sollner, C. *et al.* Mutations in cadherin 23 affect tip links in zebrafish sensory hair cells. *Nature* **428,** 955–959 (2004).
37. Michaely, P., Tomchick, D. R., Machius, M. & Anderson, R. G. Crystal structure of a 12 ANK repeat stack from human ankyrinR. *EMBO J.* **21,** 6387–6396 (2002).
38. Kachar, B., Parakkal, M., Kurc, M., Zhao, Y. & Gillespie, P. G. High-resolution structure of hair-cell tip links. *Proc. Natl Acad. Sci. USA* **97,** 13336–13341 (2000).
39. Ricci, A. J., Wu, Y. C. & Fettiplace, R. The endogenous calcium buffer and the time course of transducer adaptation in auditory hair cells. *J. Neurosci.* **18,** 8261–8277 (1998).
40. Hudspeth, A. J., Choe, Y., Mehta, A. D. & Martin, P. Putting ion channels to work: mechanoelectrical transduction, adaptation, and amplification by hair cells. *Proc. Natl Acad. Sci. USA* **97,** 11765–11772 (2000).
41. Starr, C. J., Kappler, J. A., Chan, D. K., Kollmar, R. & Hudspeth, A. J. Mutation of the zebrafish choroideremia gene encoding Rab escort protein 1 devastates hair cells. *Proc. Natl Acad. Sci. USA* **101,** 2572–2577 (2004).
42. He, T. C. *et al.* A simplified system for generating recombinant adenoviruses. *Proc. Natl Acad. Sci. USA* **95,** 2509–2514 (1998).

Supplementary Information accompanies the paper on **www.nature.com/nature**.

Acknowledgements Authors' contributions are listed in Supplementary Information. We thank C.-L. Chen and Q. Ma for assistance with *in situ* hybridization, N. Hopkins for zebrafish support and L. Stevens for laboratory administration. This work was supported by grants from NIH to N. Hopkins, S.-Y.L., J.G.-A., G.S.G.G., J.R.H. and D.P.C.; from the Mathers Foundation to D.P.C.; from the Howard Hughes Medical Institute (J.G.-A.); and from the Charles Dana Foundation to Q. Ma. P.G. was a Parker B. Francis Fellow in Pulmonary Medicine. J.G.-A., A.D., G.G., J.R.H. and H.L.R. were Associates, M.A.V. and K.K. are Associates, and D.P.C. is an Investigator of the Howard Hughes Medical Institute.

Competing interests statement The authors declare that they have no competing financial interests.

Correspondence and requests for materials should be addressed to D.P.C. (dcorey@hms.harvard.edu).